TH/P3-14

Gyrokinetic Simulation of Energetic Particle Turbulence and Transport

L. Chen[1], A. Bierwage[1], S. Briguglio[4], M. S. Chu[2], W. Heidbrink[1], I. Holod[1], Z. Lin[1], D. Spong[3], M. A. Van Zeeland[2], G. Vlad[4], R. E. Waltz[2], Y. Xiao[1], W. Zhang[1], and F. Zonca[4]
[1]University of California, Irvine, CA 92697, USA
[2]General Atomics, San Diego, CA 92186, USA
[3]Oak Ridge National Laboratory, Oak Ridge, TN 37831, USA
[4]EURATOM-ENEA, Cassella Postale 65-00044 Frascati, Italy
Email contact of main author: liuchen@uci.edu

Abstract. The fully self-consistent simulation of energetic particle turbulence and transport in burning plasmas such as ITER must incorporate three new physics elements: (i) kinetic effects of thermal particles at the thermal ion gyroradius (*micro* scale), (ii) nonlinear interactions of many *meso* scale (energetic particle gyroradius) shear Alfvén waves induced by the kinetic effects at the *micro* scale, and (iii) *meso-micro* couplings of the microturbulence and Alfvénic fluctuations. The large dynamical ranges of spatial-temporal processes further require global simulation codes efficient in utilizing massively parallel computers at the petascale level and beyond. Therefore, the studies of energetic particle physics in ITER burning plasmas call for a gyrokinetic turbulence approach. Progress of gyrokinetic simulations of energetic particle turbulence and transport in tokamaks is reported in this paper. Specifically, nonlinear gyrokinetic simulations find that the energetic particle transport induced by the microturbulence decreases rapidly due to the averaging effects of the large gyroradius and banana width, and the fast decorrelation of energetic particles with waves. Linear global gyrokinetic simulations using GTC and GYRO demonstrate the excitation of the toroidal Alfvén eigenmode (TAE) by the pressure gradient of the energetic particles. The TAE linear dispersion from gyrokinetic simulations is in reasonable agreement with conventional fluid simulations. Furthermore, initial linear and nonlinear simulations of a DIII-D experiment dedicated for energetic particle studies find fast ion instabilities.

1. Introduction

Energetic particles can be generated in magnetically confined plasmas by fusion reactions and auxiliary heating. They are subjected to the diffusion by macroinstabilities [1], microturbulence [2], stochastic magnetic fields [3], and classical collisional and orbital effects [4]. The confinement of energetic particles is a critical issue in the International Thermonuclear Experimental Reactor (ITER) [5], since the ignition relies on the self-heating by energetic fusion products. In ITER burning plasma experiments, energetic particles will constitute a significant fraction of the local plasma energy density [6]. Since such energetic populations often exist in states far away from thermal equilibrium due to their non-Maxwellian distribution and/or peaked pressure profiles at the core, they can readily tap the corresponding free energy and collectively excite electromagnetic instabilities to intensities much enhanced over thermal levels. The intrinsic time and length scales of these instabilities leads to a breakdown of the constants of motion and a resultant enhanced level of transport in the corresponding phase space (mainly, energy and radius) of energetic particles, which could adversely affect the overall performance of ITER experiments [7,8].

Among the various plausible collective electromagnetic instabilities in burning plasmas, the shear Alfvén wave (SAW) has long been theoretically recognized and experimentally verified as the most prominent one. The SAW instability, e.g., toroidal Alfvén eigenmode (TAE) [1] and energetic particle mode (EPM) [9], is most dangerous to energetic particle confinement. It excites short wavelength fluctuations that maximize tapping of the pressure gradient free energy and drive symmetry-breaking transport. It has the unique feature of having a nearly constant group velocity along the confining magnetic field, similar to that of energetic

particles, thus rendering wave-particle resonance accessible to a large fraction of the energetic particles. Intensive theoretical and experimental research (see Ref. 6 for a review), as well as numerical simulations [10-14] over the last two decades has clearly delineated the important aspects of the linear physics of SAW instabilities: wave spectra, excitation mechanisms, mode structures, and damping mechanisms. The basic conclusions are: (1) SAW spectra consist of continuous spectra (due to radial inhomogeneities) with finite gaps (due to equilibrium symmetry breakings) at frequencies ranging from Alfvén to thermal ion transit frequencies; (2) two types of modes may exists [7-9,15], i.e., discrete Alfvén eigenmodes (AEs) inside the gaps due to background equilibrium and/or energetic particle effects, and EPMs that are excited at the fast particle characteristic frequencies when the mode drive overcomes continuum damping; (3) instability excitation maximizes when the wavelength perpendicular to the confining magnetic field is comparable to the energetic particle's gyroradius ρ_E (defined as ***meso*** scale); and (4) the instability has thresholds that are imposed by damping from both thermal ions and trapped electrons. In particular, there is significant damping via local/global resonant mode conversion due to kinetic effects of thermal ions to kinetic Alfvén waves with radial wavelengths comparable to the thermal ion gyroradius ρ_i (defined as ***micro*** scale) and finite parallel electric field. Although these key linear physics mechanisms have been identified, a global, fully self-consistent, nonlinear kinetic code is desirable to simultaneously resolve *micro* and *meso* scales to reliably map out the linear stability boundaries and to accurately predict the nonlinear saturation amplitude for realistic ITER plasma parameters and equilibria.

Effects of collective SAW instabilities on the energetic particle confinement depend ultimately on the self-consistent nonlinear evolution of SAW fluctuations. Here, physical insight and understanding will require computations on a truly grand challenge scale. The complexities of nonlinear dynamics are further compounded by the complexities of geometries (e.g., radial inhomogeneities and equilibrium symmetry breakings) intrinsic to SAW in tokamak plasmas. Consequently, the current knowledge on energetic particle-induced SAW nonlinear physics and transport remains isolated and qualitative. Specifically, the nonlinear evolution of SAW turbulence depends critically on the complex nonlinear phase space dynamics of energetic particles [16] as well as on the complex nonlinear mode-mode couplings among the multiple SAW modes [8] that are expected in ITER plasmas. Both nonlinear effects, in turn, depend sensitively on the global features of wave-particle resonances and mode structures. Current understanding is typically based on the reduced models of a single toroidal SAW mode with a single wave-particle resonance and/or an isolated nonlinear mode-coupling effect; e.g., zonal flow/field [17,18] or nonlinear frequency gap modification [8]. These reduced models based on a coherent mode or non-interacting modes often predict a transport of energetic particles well below the level observed in experiments. Recognizing that SAW instabilities in ITER plasmas will typically be comprised of modes with toroidal mode numbers $n \sim 20 \sim O(a/\rho_E)$ (a is the minor radius) and that for each n, there are $O(n)$ frequency gaps within which SAW modes may be localized, the current understanding is far from being adequate. Therefore, it is necessary to develop nonlinear kinetic codes for simulation of *meso*-scale energetic particle turbulence, which incorporates all the essential physics mechanisms including kinetic thermal particles and, must be able to efficiently handle a large number of interacting SAW modes.

More challenging still are the physics of couplings between energetic particle-induced SAW turbulence and microscopic drift-Alfvén wave (DAW) turbulence driven by thermal particles [7,19,20], which is ubiquitous in fusion plasmas. Recognizing that DAW turbulence has frequencies comparable to the lower end of SAW turbulence but *micro*-scale perpendicular

wavelengths, e.g., $n\sim200\sim O(a/\rho_i)$ could be expected for DAW turbulence in ITER plasma, a unified simulation platform self-consistently treating both *meso*- and *micro*-turbulence is obviously needed to examine the energetic particle transport due to DAW turbulence and thermal particle transport due to SAW turbulence. The fully self-consistent simulation of energetic particle turbulence and transport must therefore incorporate three new physics elements: kinetic effects of thermal particles, nonlinear interactions of a large number of *meso*-scale modes, and cross-scale couplings of *meso-micro* turbulence. The large dynamical ranges of spatial-temporal processes further require global simulation codes that are efficient in utilizing massively parallel computers at the petascale level and beyond. Therefore, the studies of energetic particle physics in ITER burning plasmas require a kinetic turbulence approach. Since the important SAW frequencies (e.g., TAE and EPM) are much smaller than the ion cyclotron frequency, the most suitable method for this new paradigm is nonlinear gyrokinetics, which removes unwanted high frequency modes and rigorously retains all linear and nonlinear wave–particle resonances and finite Larmor radius effects.

Progress of gyrokinetic simulations of energetic particle turbulence and transport in tokamaks is reported in this paper. Specifically, nonlinear gyrokinetic simulations find that the energetic particle transport induced by the microturbulence decreases rapidly due to the averaging effects of the large gyroradius and banana width, and the fast decorrelation of energetic particles with waves. Linear global gyrokinetic simulations using GTC [21] and GYRO [22] demonstrate the excitation of TAE by the pressure gradient of energetic particles. Linear dispersion from gyrokinetic simulations is in reasonable agreement with conventional fluid simulations. Furthermore, initial linear and nonlinear simulations of a DIII-D experiment dedicated for energetic particle studies find fast ion instabilities. In Sec. II, we discuss gyrokinetic simulation of the TAE excitation by energetic particles. Energetic particle transport by microturbulence is presented in Sec. III.

2. Gyrokinetic simulation of TAE excitation by energetic particles

Gyrokinetic simulations of Alfvénic waves that are driven unstable by energetic particles have been performed using particle code GTC and continuum code GYRO. In initial GTC simulations [23], continuum damping of the SAW has been demonstrated and a frequency gap due to the toroidal effects has been generated. In the presence of the energetic particle density gradient, the excitation of the toroidal Alfvén eigenmode (TAE) has been observed with a frequency residing inside the gap. Initial GYRO simulations with a small cyclic flux tube have shown high-n TAE modes driven by the energetic particle resonance. The modes are most unstable inside the expected frequency gap. Large cyclic flux tubes (across the whole plasma with many singular surfaces) simulations give similar results. These preliminary simulations have demonstrated the feasibility of gyrokinetic approach for simulating energetic particle driven Alfvén instabilities.

GYRO is a physically comprehensive and extensively benchmarked code for the solution of nonlinear gyro-kinetic-Maxwell equations. Electrons are fully drift-kinetic and transverse electromagnetic fluctuations are included. Equilibrium profile variations are allowed over an arbitrary radial annulus. In the simulation using the s-α flux tube equilibrium, background plasma density and temperature gradients are set to zero and energetic particles have a Maxwellian distribution function with a thermal velocity matching the velocity of Alfvén waves. The mode frequencies from simulations fall within the predicted TAE gap. The parallel electric field ($E_{||}$) is small as predicted by the MHD theory. Extensive simulations using this s-α geometry show that the dependence of the frequency (ω) and the growth rate

(γ) on all following parameters follows that predicted by the known MHD theories: the poloidal wave number (k_θ), the density (n_h) and density gradient (dn_h/dr) of the energetic particles, the safety factor (q), the magnetic shear ($r/q\ dq/dr$), and the β values of background plasmas. We have also performed simulations using a thin flux tube with cyclic boundary conditions. These simulations show that the growth rates of a thick flux tube with zero boundary condition differ only slightly from those using cyclic boundary conditions. The relationship between TAE frequency and growth rate is summarized in Fig. 1. The colored band is the range of frequency bounded by the Alfvén continuum and the dots sweep though various low n-numbers. Clearly, the computed TAE growth rates are higher when the frequencies fall within the gap and are markedly smaller when outside.

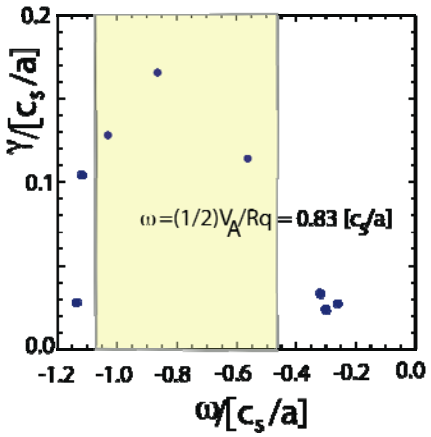

Fig. 1. Linear growth rate as a function of real frequency in GYRO simulation of TAE mode.

Verification-- To verify the gyrokinetic simulation of toroidal SAW eigenmodes, benchmark cases have been designed for code comparisons using a suite of nonlinear turbulence codes, as well as linear eigenvalue and initial-value codes. For verification, a circular, low β, R_0/a = 3 tokamak equilibrium, and a parabolic profile with $q(0)$ = 1.3, q(a) = 3.9 are chosen. The energetic particle parameters that are fixed are the ratio of the energetic particle velocity to the Alfvén velocity, v_{EP}/v_A = 1, and the density gradient scale length, a/L_{EP} = 8 with a peak value near r/a = 0.5. Maxwellian distributions are assumed for energetic particles. The profiles for thermal ions and electrons are chosen as constant in radius in order to avoid exciting secondary drift instabilities. We retain the toroidal mode number, n, and the central fast ion $\beta_{EP}(0)$ as independent varying parameters. Typically, n is varied over a range of 3 to 10 and β_f from 0.01 to 0.04. Both gyrokinetic GTC and hybrid TAEFL [11] find unstable TAE modes with real frequencies in the lowest order gap and growth rates that are close (±20%) over certain ranges of n and $\beta_{EP}(0)$, as shown in Fig. 2 for n=3 mode.

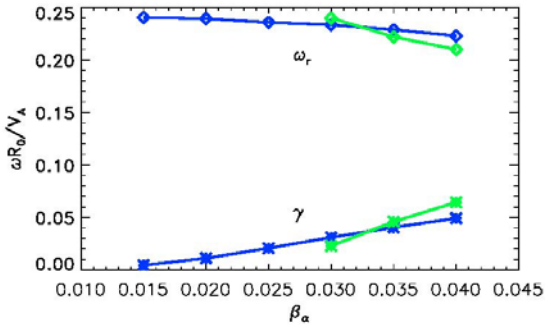

Fig. 2 TAE real frequency and growth rate from GTC (green) and TAEFL simulation (blue).

Validation-- A DIII-D shot #122117 [24,25] which is exceptionally well-diagnosed and extensively studied is chosen for comparisons with gyrokinetic and hybrid simulation codes. The simulation of this experiment is challenging for both the SAW modes and the associated energetic particle transport. The simulation must confront the coexistence and interaction of a spectrum of at least two types of Alfvénic modes, namely TAE and reverse shear Alfvén eigenmode (RSAE) [26]. Measured temperature perturbations are of similar peak magnitude for both types of modes. Predictions of the temperature perturbation from the ideal MHD code NOVA [27] is in close agreement with measurements. However, straightforward application of the ORBIT code [28] without the mode frequency sweep cannot match the experimentally observed energetic particle transport. In support of modeling efforts, dedicated DIII-D time was given to obtain a circular version of the discharge #122117. The new discharge (shot #132707) [29] was extremely successful and took advantage of recent diagnostic upgrades with simultaneous measurements of density and temperature fluctuations across a significant fraction of the plasma radius for the entire shot duration.

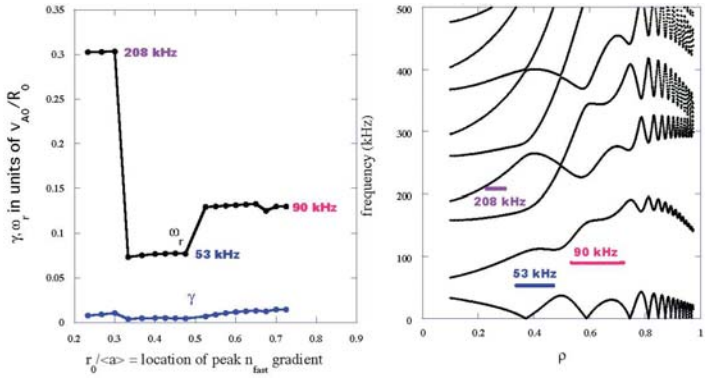

Fig. 3 *Linear dispersion and frequency gap structure from TAEFL simulation of DIII-D shot #122117.*

TAEFL [11] is utilized to simulate the energetic particle driven AE modes in the DIII-D shot #122117, which is D-shaped with a reversed shear q-profile having $q_{\min} \approx 4.2$. TAEFL is an initial-value, reduced MHD fluid-kinetic hybrid model for arbitrary non-circularly shaped tokamak configurations. Gyrofluid closure methods are used to include the wave-particle coupling physics required to excite energetic particle-driven instabilities. A scan in fast ion density profile shapes (i.e., stepping the peak gradient location from the center to the edge) was made for n=3 modes that illuminates the range of unstable AE modes. As Fig. 3 shows, 3 modes (EAE at 208 kHz, RSAE at 53 kHz, TAE at 90 kHz) were found by this scan. These identifications are based on the dominant mode couplings present in the eigenfunctions. Of these, the RSAE and TAE are consistent with the frequency range of coherent modes that were observed. Small variations in the q-profile used in the TAEFL equilibrium for the RSAE case indicated that the RSAE converts to a TAE for q=4.15 and 4.4. These changes in mode structure are accompanied by large (~ factor of 2) upshifts in the real frequency of the mode. Such frequency upshifts were also observed experimentally.

DIII-D discharge #132707 is a nearly circular cross-section case and a reversed shear profile with $q_{min} \approx 2$. In GYRO simulations using experimental geometry and profile, background plasma density and temperature gradients are first zeroed out. An analytically prescribed density distribution function for the energetic particles with a peaked density gradient localized around r/a=0.6 is adopted. The eigenfunction for the perturbed potential of n=4 mode (Fig. 4) shows coupling of poloidal harmonics typical of TAE modes. We also found that growth rate is not significantly affected by the background temperature gradient but could be stabilized by the background density gradient.

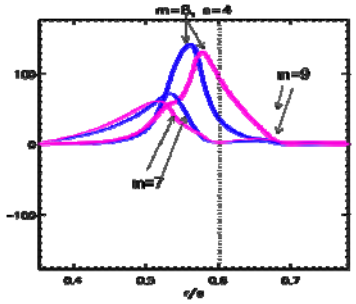

Fig. 4 Radial profile of TAE mode poloidal harmonics in GYRO simulation of DIIID shot #132707.

Using the experimental profiles and parameters of shot #132707, TAEFL scans in fast ion pressure were carried out for n=2 to 8. For n=2-4, RSAE instabilities are found with real frequencies just above the lower continuum near the $q_{\min}$ location as shown for n=3 in Fig. 5. The mode structure for these instabilities is dominated by a single poloidal mode number with m=2n. For n=5–8, TAE instabilities are present with broader coupled poloidal mode spectra and with real frequencies about twice as large as the RSAE modes.

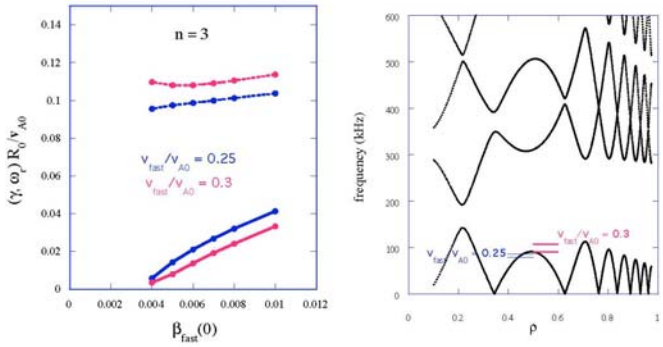

Fig. 5 Real frequency, growth rate, and frequency gap structure of n=3 mode from TAEFL simulation of DIII-D shot #132707.

HMGC [12] simulations based on shot #132707 (t=725ms) have been performed. Preliminary results show fast-ion-driven instabilities of n=6 mode and γ/ω_r~0.1, which cause no significant redistribution of fast ions [FIG. 6 (a)], as is expected for a stable experimental profile. In the nonlinearly saturated stage, continuing Alfvénic activity is seen near $q_{\min}$ [FIG. 6 (b)]. We performed two simulations with slightly different $q_{\min}$ for sensitivity studies.

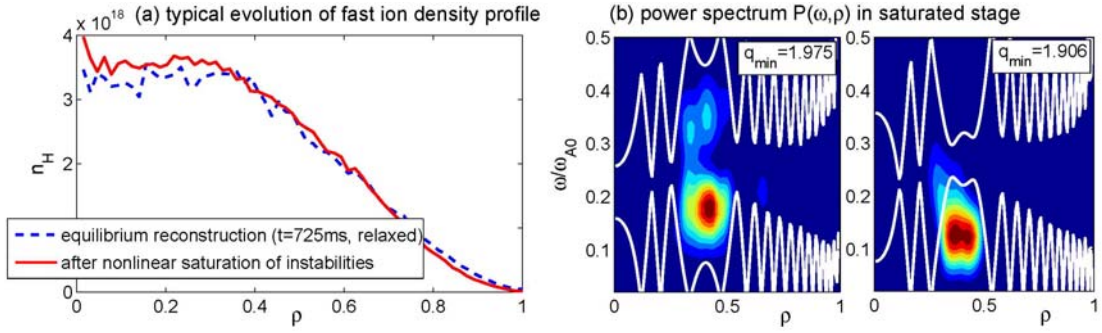

Fig. 6 HMGC results for DIII-D shot 132707, t=725ms. (Panel a): Radial fast ion density profile at the beginning of the simulation and after nonlinear saturation of the instabilities. (Panel b): Power spectrum $P(\omega,\rho)$ shows mode activity near q_{min} (ρ=0.4) after nonlinear saturation. The white lines indicate the Alfvén continuum and two examples with different values of q_{min} are shown.

3. Energetic particle transport by microturbulence

Earlier fusion experimental [4,30] and theoretical [31] studies indicated that energetic particles do not suffer a large transport due to the microturbulence excited by the pressure gradients of thermal particles. However, a recent fusion experiment [32] showed some evidence of the correlation between the excitation of the microturbulence and the redistribution of energetic ions produced by the neutral beam injection (NBI). Some recent theoretical [33] and computational [34] studies also suggested a significant transport level of the energetic particles driven by the microturbulence. To resolve this discrepancy, here we study the diffusion of the energetic particles by the microscopic ion temperature gradient (ITG) [2] turbulence in large scale first-principles simulations of fusion plasmas using the global GTC [21]. The fast ion radial spread as a function of energy and pitch angle is measured in the steady-state ITG turbulence. The probability density function of the radial excursion is found to be very close to a Gaussian, indicating a diffusive transport from a random walk process. The radial diffusivity as a function of the energy and pitch angle can thus be calculated using the random walk model. We find [35] that the diffusivity decreases drastically for high energy particles due to the averaging effects of the large gyroradius and banana width, and the fast decorrelation of the energetic particles with the ITG oscillations. By performing the integration in phase space, we can calculate the diffusivity for any distribution function. The NBI ion diffusivity driven by the ITG turbulence is found to decrease rapidly for the born energy up to an order of magnitude of the plasma temperature and more gradually to a very low level for higher born energy. This result may explain the differences between the older experiments [4] with a higher born energy and the newer experiment [32] with a lower born energy (relative to the plasma temperature). The GYRO simulation [34] also found some re-distribution of the α-particles away from the classical slowing down in the ITG/TEM (trapped electron mode) turbulence and both positive and negative fast particle (density and energy) flows in the presence of kinetic electrons.

In GTC simulation of ITG turbulence, we measured the radial excursion of several group of ions in phase space. We calculate the mean-squared radial displacement of each group of particles $\left\langle \Delta r^2 \right\rangle = \frac{1}{N}\sum_{i=1}^{N}\left[r_i(t)-r_i(0)\right]^2$, where $r_i(0)$ and $r_i(t)$ are the radial position of the ith particle at time t=0 and time t, respectively. To isolate the effects of turbulence scattering, we also calculate the equilibrium radial displacements of the same ions in another simulation where the ITG turbulence is suppressed. The equilibrium displacements are identical to the perturbed displacements for all energy groups before the turbulence grows to a high amplitude. After the turbulence reach a steady state, the difference between the equilibrium and perturbed displacements is small for high energy ions (e.g., E=16T_e), indicating that the effect of the turbulence on the high energy orbits is small. On the other hand, for a lower energy (e.g., E=2T_e), the perturbed displacement is much larger than the equilibrium displacement, indicating that the effect of the turbulence scattering dominates the radial displacement. The net turbulent displacement (perturbed displacement subtracted by the equilibrium displacement) increases linearly with time for all energy groups in the steady-state ITG turbulence. This feature indicates that the radial excursion of the ions due to the turbulence scattering is a diffusive process. The probability density function (PDF) of the radial displacement for each energy group is indeed very close to a Gaussian. The diffusive nature of the ITG turbulent transport is further supported by the fact that the radial profile of the heat conductivity matches very well with the intensity profile; i.e., the transport is driven by the local fluctuation [36]. The stochastic wave-particle decorrelation [37,38] due to the overlaps of the phase-space islands gives rise to the diffusive transport process.

Since the radial excursion of the ions is diffusive, a phase-space-resolved diffusivity can be defined using the random walk model $D(E,\xi)=\frac{\Delta\sigma^2}{2\Delta t}$, where $\Delta\sigma^2$ is the change of the PDF standard deviation of the net radial displacement for each group of ions with energy E and pitch angle ξ during a time interval of Δt when the turbulence is in a steady state. The diffusivity is relatively smooth across the pitch angle ξ with no sharp resonance in the entire phase space. This is consistent with the diffusive process and the transport could therefore be described by a quasilinear theory [37,38]. As a consistency check, we calculate the diffusivity of the thermal ions by averaging the diffusivity D over a Maxwellian distribution function with a temperature of T_i, $D_0=\int DF_M d^3v$. We find that this diffusivity D_0 based on the random walk model is very close to an effective particle diffusivity D_i of thermal ions measured in the simulation, D_0 =1.1 D_i. Here $D_i = 2\chi_i/3$ and χ_i is calculated from the self-consistent heat flux using $Q_i=\int v^2\delta v_r \delta f \frac{1}{2} d^3v$ measured in the simulation, where v is particle velocity, δf is the perturbed distribution function, and δv_r is the radial component of gyrophase-averaged ExB drift. The diffusivity integrated over the pitch angle as shown in Fig. 1 peaks at the resonant energy of E=2T_e and decreases drastically for higher energy particles, due to the averaging effects of the large gyroradius and orbital width, and the fast decorrelation of the energetic particles with the waves for the high energy particles.

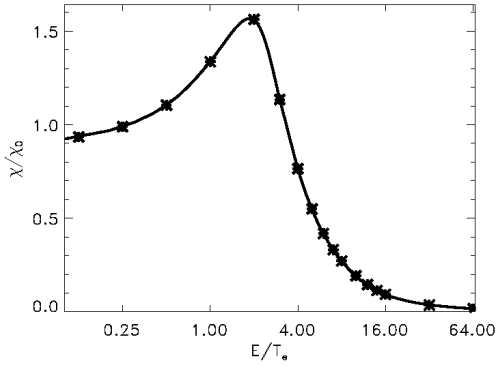

Fig. 7 Diffusivity driven by ITG turbulence for isotropic, mono-energetic particles.

To understand the mechanisms of the reduction of the energetic particle diffusivity, we examine the asymptotic scaling of the diffusivity with respect to the particle energy for specific pitch angle. We find that the diffusivity $D\propto 1/E^2$ for trapped particles with E>3T_e. This scaling can be understood from the quasilinear theory of the diffusivity for trapped particles in high energy limit, $D\propto\sum_n \frac{c^2\left|k_r k_\theta \phi_n\right|^2}{B^2} J_0^2(k_\perp\rho_E) J_0^2(k_\perp\rho_b)\delta(\omega-\omega_d+p\omega_b)$. Here the first Bessel function J_0 comes from the gyroaveraging and the second from the averaging over banana orbits, $\omega_b=\sqrt{\varepsilon}v_E/(2\pi qR)$ is the bounce frequency, ε=r/R is the inverse aspect ratio, ρ_b is the banana width, ρ_E and v_E are the gyroradius and velocity of energetic particles, respectively, k_r and k_θ are the wave number in the r and θ direction, B is the magnetic field, Φ_n is the electrostatic potential, and p is the harmonics integer number. These two averages give rise to a dependence of D on $1/E$ when taking a large argument expansion of the Bessel function. Regarding the resonance condition, since ω_d, ω_b >>ω for energetic particles, we need p>0. Therefore the resonance condition becomes ω_d=$p\omega_b$, or equivalently, $n\omega_{pre}$=$p\omega_b$, where ω_{pre}=$qE/(mRr\Omega)$ is the precession frequency. This gives rise to another dependence of

D on $1/E$ when integrating over Φ_n since ω_{pre} is proportional to E. Hence, the diffusivity $D \propto 1/E^2$ for trapped particles accounts both the orbit averaging and the decorrelation process. For passing particles, the resonance condition of $\omega=k_{||}v_{||}$ and the orbital averaging will each give rise to an $E^{-1/2}$ dependence of D, so we expect a diffusivity $D \propto 1/E$.

This work is supported by US DOE SciDAC GSEP Center.

References

[1] C. Z. Cheng, L. Chen, and M. S. Chance, *Ann. Phys.* (N.Y.) **161**, 21 (1985).
[2] W. Horton, *Rev. Mod. Phys*. **71**, 735 (1999).
[3] A. B. Rechester and M. N. Rosenbluth, *Phys. Rev. Lett*. **40**, 38 (1978).
[4] W.W. Heidbrink and G. J. Sadler, *Nucl. Fusion* **34**, 535 (1994).
[5] http://www.iter.org.
[6] A. Fasoli *et al*, *Nucl. Fusion* **47**, S264 (2007).
[7] ZONCA, F., et al., Plasma Phys. Control. Fusion **48** (2006) B15.
[8] CHEN, L., and ZONCA, F., Nucl. Fusion **47** (2007) S727.
[9] L. Chen, *Phys. Plasmas* **1**, 1519 (1994).
[10] G. Y. Fu and C. Z. Cheng, *Physics of Fluids B-Plasma Physics* **4**, 3722 (1992).
[11] D. A. Spong, B. A. Carreras, and C. L. Hedrick, *Phys. Plasmas* **1**, 1503 (1994).
[12] S. Briguglio, G. Vlad, F. Zonca, and C. Kar, *Phys. of Plasmas* **2**, 3711 (1995).
[13] Y. Todo *et al*, *Phys. Plasmas* **2**, 2711 (1995).
[14] P. Lauber et al, *J. Comput. Phys.* **226**, 447 (2007).
[15] ZONCA, F., and CHEN, L., Plasma Phys. Control. Fusion **48** (2006) 537.
[16] H. L. Berk, B. N. Breizman, and H. C. Ye, *Phys. Rev. Lett*. **68**, 3563 (1992).
[17] CHEN, L., et al., Nucl. Fusion **41** (2001) 747.
[18]P. H. Diamond et al, *Plasma Phys. and Control. Fusion* **47**, R35 (2005).
[19] F. Zonca, L. Chen, and R. A. Santoro, *Plasma Phys. Control. Fusion* **38**, 2011 (1996).
[20] R. Nazikian *et al*, *Physical Review Letters* **96**, 105006 (2006).
[21] Z. Lin *et al*., *Science* **281**, 1835 (1998).
[22] J. Candy and R. E. Waltz, *J. Comput. Phys.* **186**, 545 (2003); R.E. Waltz, J. Candy, F.L. Hinton, C. Estrada-Mila, J.E. Kinsey, Nucl. Fusion **45**, 741 (2005).
[23] Y. Nishimura, Z. Lin, and W. X. Wang, *Phys. Plasmas* **14**, 042503 (2007).
[24] M. A. Van Zeeland *et al*, *Phy. Rev. Lett*., **97**, 135001 (2006).
[25] W. W. Heidbrink *et al*, *Phy. Rev. Lett*., **99**, 245002 (2007).
[26] M. Takechi *et al.*, "*Property of Alfven eigenmode in JT-60U reversed shear and weak shear discharges*", 19th IAEA Fusion Energy Conference, 2002, Paper EX/W6.
[27] C. Z. Cheng, Phys. Reports 211, 1(1992).
[28] R. B. White and M. S. Chance, *Phys. Fluids* **27**, 2455 (1984).
[29] M.A. Van Zeeland *et al*, "*Alfvenic Instabilities and Fast Ion Transport in the DIII-D Tokamak*", 22th IAEA Fusion Energy Conference, 2008, Paper EX/6-2.
[30] S. J. Zweben *et al*, *Nucl. Fusion* **40**, 91 (2000).
[31] G. Manfredi and R. O. Dendy, *Phys. Rev. Lett*. **76**, 4360 (1996).
[32] S. Gunter et al., *Nucl. Fusion* **47**, 920 (2007).
[33] M. Vlad and F. Spineanu, *Plasma Phys. Control. Fusion* **47**, 281 (2005).
[34] C. Estrada-Mila, J. Candy, and R. E. Waltz, *Phys. Plasmas* **13**, 112303 (2006).
[35] W. L. Zhang, Z. H. Lin, and L. Chen, *Phys. Rev. Lett.* **101**, 095001 (2008).
[36] Z. Lin and T. S. Hahm, *Phys. Plasmas* **11**, 1099 (2004).
[37] I. Holod and Z. Lin, *Phys. Plasmas* **14**, 032306 (2007).
[38] Z. Lin et al., *Phys. Rev. Lett.* **99**, 265003 (2007).